Mon. Not. R. Astron. Soc. **370,** L33–L37 (2006) doi:10.1111/j.1745-3933.2006.00183.x

GRB 990413: insight into the thermal phase evolution

Z. Bosnjak,[1,2]★ A. Celotti[1] and G. Ghirlanda[2]

[1]*S.I.S.S.A., via Beirut 2-4, I-34014 Trieste, Italy*
[2]*INAF-Observatory of Brera, via Bianchi 46, I-23807 Merate (LC), Italy*

Accepted 2006 April 19. Received 2006 March 31; in original form 2005 September 9

ABSTRACT

GRB 990413 shows a very hard spectrum [with a low-energy spectral component $F(\nu) \propto \nu^{2.49}$] which is well represented by a blackbody model with characteristic temperature $\sim$70 keV. It thus belongs to the subset of gamma-ray bursts (GRBs) which might be revealing a thermal phase. We find that the temperature/luminosity evolution is consistent with that found in the other 'thermal' GRBs. The time-resolved spectral analysis indicates the presence of a second non-thermal component contributing (for about 1 s) up to 30 per cent of the total flux. Differently from the other thermal GRBs, GRB 990413 shows significantly high level of variability and the evolution of the thermal/non-thermal spectral components is strongly correlated with the flux variations. This GRB thus offers the unique opportunity to test the standard fireball photospheric and internal shock phases and their reciprocal influence. GRB 990413 was not selected on the basis of its spectrum and thus hints to the possibility that this early behaviour might be more common than currently known.

Key words: radiative processes: non-thermal – radiative processes: thermal – gamma-rays: bursts.

1 INTRODUCTION

In the 'standard' scenario, the spectrum of gamma-ray bursts (GRBs) is interpreted as synchrotron/inverse Compton radiation from relativistic electrons accelerated in internal shocks within a relativistic outflow (Rees & Mészáros 1994). The majority of the observed spectral and temporal GRB properties are fairly well interpreted within this framework. However, the nature of the prompt emission remains one of the most interesting unresolved problems related to GRB events.

In particular, the spectral parameter (e.g. in Band's parametric representation, Band et al. 1993) that is most constraining for the emission models of GRBs is the low-energy power-law (PL) photon index α. Synchrotron radiation from isotropic particle distributions (Katz 1994), as well as alternative scenarios (see e.g. Lloyd & Petrosian 2002; Mészáros & Rees 2000; Granot, Piran & Sari 2000; Ghisellini, Celotti & Lazzati 2000) predict limits on α which are consistent with at most 70 per cent of the analyzed GRB spectra (e.g. Preece et al. 2000). Radiation mechanisms other than synchrotron have been proposed: they involve Comptonization of a thermal photon/particle distributions, e.g. the Compton drag model (Lazzati et al. 2000) or quasi-thermal Comptonization model (Ghisellini & Celotti 1999; Rees & Mészáros 2005). Furthermore, the time-resolved spectral analysis revealed that the spectrum evolves with time (e.g. Ford 1995; Preece et al. 2000). This might indicate an evolution of the physical conditions of the plasma, or that various emission processes dominate at different times and/or that the spectral evolution is directly related to the physics of the central engine.

Ghirlanda, Celotti & Ghisellini (2003, GCG03 hereafter), focusing on the time-resolved spectral analysis of a handful of extremely hard GRB spectra, enlightened the difficulties of accounting for the non-thermal models and suggested that in some bursts the initial emission phase could have a thermal character. More recently, Ryde (2004, R04 hereafter) studied a few GRBs with very hard spectra, discussing the observed emission in terms of two spectral components, i.e. a blackbody (BB) and a PL, which showed relative variable strengths throughout the burst durations.

In fact, in the standard GRB model (e.g. Mészáros & Rees 2000; Daigne & Mochkovitch 2002) a thermal spectrum is predicted to appear when the fireball becomes transparent (see the above references for alternative scenarios). Initial thermal emission does not exclude the presence of a non-thermal contribution due to the development of internal shocks within the fireball. Therefore, we should expect to find GRBs where both thermal and non-thermal components are present and might evolve differently due to their different origins (e.g. Rees & Mészáros 2005).

In this paper we report the finding (by chance) of a new hard burst, GRB 990413, which is particularly interesting for its spectral and temporal properties. The emission of GRB 990413 is consistent with a thermal BB spectrum for the whole of its duration (not only during the initial phase) and, differently from the other cases of 'thermal bursts', its light curve shows a high level of variability. The finest time-resolved spectral analysis reveals the presence of an underlying non-thermal emission component and shows that the

★E-mail: bosnjak@sissa.it

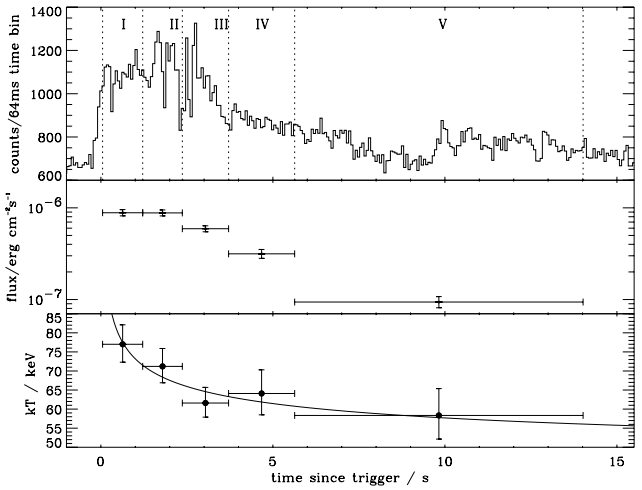

Figure 1. Top: GRB 990413 light curve summed over the four BATSE energy channels ($E > 25$ keV). The five time-intervals for which the time-resolved spectral analysis was performed are indicated (see Table 1). Middle: best-fitting BB model flux integrated in the energy fit range. Bottom: BB temperature evolution and the fit with a kT $\propto t^{-1/4}$ function (solid line).

spectral evolution of the thermal and non-thermal components is correlated with the light curve variability. We present the overall characteristics and the time-integrated properties of GRB 990413 in Sections 2 and 3. The analysis and results on its spectral evolution and its correlation with the observed light curve variability are the content of Sections 4 and 5, respectively.

2 GRB 990413

GRB 990413 was detected by BATSE.[1] It has a total fluence of $(6.813 \pm 0.449) \times 10^{-6}$ erg cm^{-2} in the energy range > 25 keV. Its duration is $T_{90} = 12.73 \pm 0.45$ s and its peak flux (integrated in the range 50–300 keV) is 3.77 ± 0.29 photons cm^{-2} s^{-1}, reached ~ 2.8 s after the trigger. These duration and peak flux are consistent with those typical of the long BATSE GRB population (e.g. Paciesas et al. 1999). The 64-ms resolution time profile integrated over the four BATSE energy channels (i.e. for energies > 25 keV) consists of two separate broad pulses (Fig. 1, top) with superimposed substructures of width $\approx$10 per cent of the main pulse width. The broad pulses (visually examined) span over the time-intervals 0–8 s and 10–14 s after the trigger.

3 TIME-INTEGRATED SPECTRUM

The spectral analysis was performed on the High Energy Resolution Burst (HERB), data[2] which are typically composed by 120 energy channel spectra distributed in the range $\sim$30–1500 keV, and have a rate-dependent accumulation time. The spectra were selected from the most illuminated Large Area Detector (LAD #5) in order to have the highest signal-to-noise (S/N) ratio (e.g. Band et al. 1993). The background spectrum was estimated as the average spectrum over two time-intervals before and after the burst trigger (2070 and 19 s, respectively).

The count spectrum, accumulated over the GRB total duration of 14 s after the burst trigger, was fitted with the Band model, i.e. parametrized by a smoothly connected double PL with low- and high-energy spectral indices α and β, and a break energy E_b (Band et al. 1993; Preece et al. 2000). This model fit resulted in $\chi^2_r = 1.27$ for 95 d.o.f., with an extremely hard low-energy spectral slope, i.e. $\alpha = 1.52^{+0.32}_{-0.30}$, and an unconstrained β due to the low signal above $\sim$600 keV. We therefore adopted the COMP model (i.e. Comptonization model), represented by a PL with a high-energy exponential cut-off $N(E) = K(E/1\,\mathrm{keV})^{\alpha} e^{-E/E_b}$, to fit the spectrum (Fig. 2).[3] With this model the reduced $\chi^2_r = 1.25$ for 96 d.o.f. was formally obtained; the COMP model best fit also indicated a very hard low-energy spectral component, with photon spectral index $\alpha = 1.49^{+0.34}_{-0.27}$, and an e-folding energy $E_b = 75.2^{+5.1}_{-5.0}$ keV, which corresponds to a peak energy $E_{peak} = E_b(\alpha + 2) \approx 260$ keV in the $E\,F_E$ spectrum.

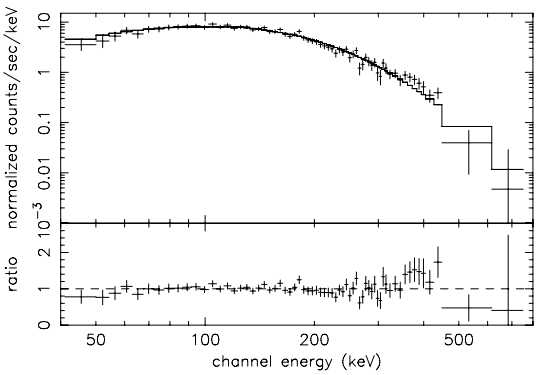

Figure 2. COMP model fit to the time-integrated (14 s) count spectrum. The solid line represents the best-fitting model with $\alpha = +1.49^{+0.34}_{-0.27}$ and $E_b = 75.2 \pm 5.0$. The lower panel shows the model-to-data ratio.

As a possible test of the consistency with the synchrotron model, we also fitted the spectrum with a COMP model with frozen low-energy spectral photon index $\alpha = -2/3$, i.e. the limiting value of the optically thin synchrotron emission (Tavani 1996). The fit resulted in a reduced $\chi^2_r \sim 4$ for 97 d.o.f., rejecting the model at the 99.9 per cent confidence level.

Given the extreme hardness of the low-energy spectral component, we fitted the time-integrated spectrum of GRB 990413 with a BB model. The best fit ($\chi^2_r = 1.27$ for 97 d.o.f.) corresponds to a temperature $kT = 67.9^{+2.3}_{-2.3}$ keV, i.e. a peak energy $E_{peak} \sim 196$ keV. This value is consistent with the peak energies of a few hundred keV found in the other 10 GRBs that are found (so far) to be consistent with thermal spectra (GCG03 and R04). We also note that, although the GRB spectrum is fitted well by a BB model, its low energy slope is slightly steeper than the Rayleigh–Jeans extrapolation in the low energy domain (i.e. $\alpha = 1$), as already indicated by the best COMP fit which gives $\alpha \sim 1.5$.

Following the procedure described in GCG03 we also tested the robustness of the spectral fits. To this aim: (i) we performed the fits reducing the energy range at the high-energy end to assess whether the characteristic exponential cut-off energy of the COMP model might determine a hard low-energy spectral component and we found that α did not significantly change within the confidence interval centred around the above best-fitting value; (ii) we examined the (null) influence of different background spectra by choosing different time-intervals to compute the average background; (iii) we used the data from the second-ranked LAD (# 7). The spectral fit

[1] http://cossc.gsfc.nasa.gov/batse/BATSE_Ctlg/index.html
[2] ftp://cossc.gsfc.nasa.gov/compton/data/batse/trigger

[3] The energy range of the fit was 43–1787 keV; the low-energy end is not the standard 30 keV as we had a large energy channel width (8 keV) at 32 keV after the channel grouping to obtain a higher S/N ratio.

resulted in a still positive, but less steep, $\alpha = 0.29^{+0.06}_{-0.28}$. Because of the lower S/N ratio in this case, $\chi^2_r = 1.61$ for 97 d.o.f.; (iv) as a check of the possible dependence on the detector response, we used the detector response matrix (DRM) corresponding to another GRB to fit the spectrum of GRB 990413. To this purpose we searched for a GRB with approximately the same angle of incidence and sky position and adopted its DRM to fit the spectrum of GRB 990413. The fit with the COMP model gives $\alpha = 1.11^{+0.27}_{-0.19}$, with $\chi^2_r = 1.26$ for 97 d.o.f. We conclude that the result that GRB 990413 has an extremely hard low-energy spectrum, consistent with a BB model, is indeed robust.

4 TIME-RESOLVED SPECTRAL ANALYSIS

As is well known, the GRB spectrum typically evolves in time with no unique behaviour. The spectral evolution is evident in all of the three spectral parameters, i.e. low- and high-energy spectral slopes and peak energy. For instance, the asymptotic α evolves in 58 per cent of the bursts (Crider, Liang & Smith 1997). Also, the GRBs with a thermal spectrum show evidence of a spectral evolution which is well described by the best-fitting temperature. GCG03 found that in their five GRBs the BB temperature, after an initial constant phase (of a few tenths of a second), evolves as $\sim t^{-1/4}$. A slightly steeper decay, $\sim t^{-2/3}$, was found in five other 'thermal' bursts by R04. The luminosity evolution instead does not show a unique behaviour.

We performed a time-resolved spectral analysis using HERB data (see Table 1), covering the time-interval 0.05–14 s after the trigger time, for a total of five spectra with similar integration time ($\sim$1.2 s each, except the last one). We fitted them with both the COMP and the BB model. The results are shown in Table 1. The reduced χ^2_r is acceptable in almost all cases (a possibly larger value is found only for the last spectrum which is indeed characterized by a lower S/N ratio). The typical values of α for the COMP model are similar to that found from the analysis of the time-integrated spectrum (i.e. $\alpha \sim 1.5$ – Section 2). Only the second spectrum shows a slightly softer low-energy spectral component (see Section 3 for a possible explanation). The peak spectral energy $E_{\rm peak}$ decreases from an initial value of $\sim$296 keV to $\sim$222 keV in the late time spectrum, indicating a typical hard-to-soft evolution.

In Fig. 1 (middle and bottom panels) we report the evolution of the spectral parameters of the BB fit (see $kT_{\rm BB}$ in Table 1). The BB flux (integrated in the fit energy range) is nearly constant for the initial 2.36 s and then decreases approximately as $\propto t^{-1}$. The temperature evolution is instead well described by $kT \propto t^{-1/4}$ (solid line in the bottom panel of Fig. 1). This behaviour fully agrees with what found by GCG03 for their set of 'thermal' GRBs.

The 10 BATSE GRBs that have spectra consistent with a thermal model present a smooth light curve (see GCG03 and R04, fig. 3 and fig. 1, respectively). GRB 990413 instead is quite variable, with a light curve characterized by rapid dips (see Fig. 4, later) during which the count rate is reduced by a factor of $\sim$3 with respect to its value at the peaks. With the aim of understanding what is happening to the thermal component during such rapid drops in intensity, we examined the spectral evolution on (even shorter) timescales, comparable with the light-curve variability.

However, the LAD data have a maximum (S/N ratio limited) time resolution $>$1 s. For this reason we analyzed the medium-energy resolution (MER) data that have a minimum accumulation time of 16 ms, despite a lower energy resolution (16 energy channels) compared to the HERB spectra. We integrated the spectra in time-bins tracking the 'peaks' and 'dips' of the light curve; the selected time-intervals are shown in Fig. 3, top panel, and reported in the first column of Table 2.

For all the spectra, in 15 selected time intervals, we first tested the BB model, and found that it does still give acceptable fits, except for those corresponding to the four 'dips' identified in the light curve. In these latter cases we found that the spectrum is best fitted by a single PL model. This appears to suggest the presence of a second non-thermal spectral component. Indeed the known GRBs with evidence of thermal spectra exhibit a smooth, continuous evolution in time,

Table 1. Results of the time-resolved spectral analysis of GRB 990413. The COMP and BB best-fitting spectral parameters are reported for each time-resolved spectrum. Errors on the parameters correspond to the 90 per cent confidence level. $\Delta t_{\rm fit}$ is the time interval over which each spectrum is accumulated. The energy fit range is approximately 40–1800 keV for all cases, except for the second spectrum which was analyzed on the reduced energy range 40–900 keV, due to the extremely low count number in the high-energy channels.

$\Delta t_{\rm fit}$ [s]	Model	α	$E_{\rm b}$ [keV]	kT$_{\rm BB}$ [keV]	$\chi^2_{\rm r}$/d.o.f.
0.05–1.21	COMP	$1.50^{+0.47}_{-0.53}$	$84.7^{+15.7}_{-8.3}$		1.17/88
	BB			$77.0^{+5.1}_{-4.7}$	1.17/89
1.21–2.36	COMP	$0.81^{+0.42}_{-0.50}$	$109.1^{+43.6}_{-21.6}$		1.04/73
	BB			$71.2^{+4.7}_{-4.3}$	1.10/74
2.36–3.71	COMP	$1.51^{+0.74}_{-0.56}$	$67.8^{+19.3}_{-8.4}$		0.85/87
	BB			$61.6^{+4.1}_{-3.7}$	0.85/88
3.71–5.63	COMP	$1.53^{+0.58}_{-0.68}$	$69.7^{+24.4}_{-10.3}$		1.04/99
	BB			$64.1^{+6.2}_{-5.6}$	1.03/100
5.63–14.01	COMP	$1.55^{+0.47}_{-0.17}$	$62.5^{+8.2}_{-5.8}$		1.36/104
	BB			$58.3^{+7.0}_{-6.2}$	1.36/105

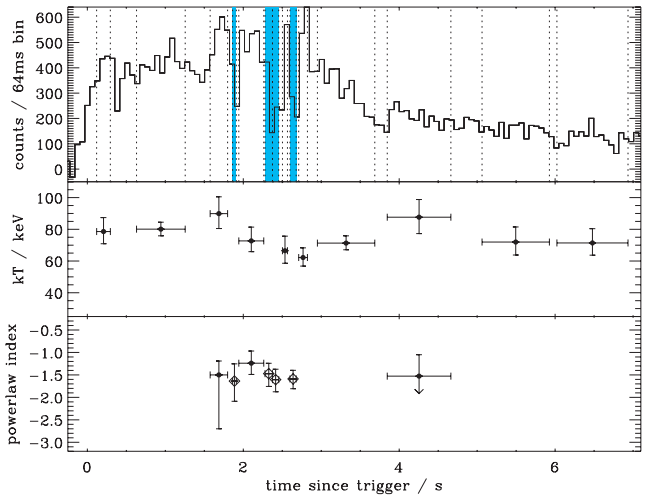

Figure 3. Results of the spectral analysis of GRB 990413 with high temporal resolution. For clarity only the first pulse of the light curve and its decay are shown; the second pulse is integrated in only one spectrum in the interval 9.9–11.3 s (due to the lower S/N ratio) as reported in Table 2. Top panel: count rate integrated over the four BATSE energy channels. The shadowed regions highlight the 'dips' of the light curve where a non-thermal contribution dominates. Middle and bottom panels: temporal evolution of the spectral parameters. Diamonds indicate the parameters corresponding to the dips. When both kT of the BB fit and the PL index are reported for the same time interval, a two-component model gave the best fit.

Table 2. Results of the spectral analysis with high temporal resolution for BB and PL models fitted to the MER data of GRB 990413. When only kT is reported, the spectrum was best fitted by a BB component alone. $\Delta t_{\rm fit}$ is the time interval over which the spectra were integrated. The energy fit range is approximately 36–1548 keV for all spectra. p is the single PL photon spectral index, defined as $N(E) \propto E^p$.

$\Delta t_{\rm fit}$ [s]	p	$kT_{\rm BB}$ [keV]	$\chi^2_{\rm r}$/d.o.f.	peak/dip
0.12–0.29	–	$78.6^{+8.8}_{-7.7}$	1.51/11	peak
0.63–1.25	–	$80.1^{+3.4}_{-4.2}$	1.73/11	peak
1.57–1.78	$-1.5^{+0.3}_{-1.2}$	$89.9^{+10.6}_{-9.4}$	1.31/9	peak
1.86–1.91	$-1.6^{+0.4}_{-0.4}$	–	0.46/10	dip
1.94–2.26	$-1.2^{+0.3}_{-0.3}$	$72.9^{+8.5}_{-6.8}$	0.78/9	peak
2.28–2.37	$-1.5^{+0.2}_{-0.3}$	–	1.26/9	dip
2.37–2.45	$-1.6^{+0.2}_{-0.3}$	–	0.77/11	dip
2.50–2.57	–	$66.5^{+9.2}_{-7.9}$	0.99/11	peak
2.59–2.68	$-1.6^{+0.2}_{-0.2}$	–	1.45/11	dip
2.71–2.82	–	$62.2^{+6.1}_{-5.4}$	1.43/11	peak
2.95–3.69	–	$71.3^{+4.6}_{-4.2}$	1.57/11	peak
3.85–4.66	$-1.5^{+0.5}_{-3.2}$	$87.6^{+11.1}_{-10.3}$	0.29/9	peak
5.06–5.92	–	$72.0^{+9.5}_{-8.2}$	1.78/11	peak
6.02–6.93	–	$71.4^{+8.9}_{-7.7}$	1.37/9	peak
9.93–11.30	$-1.3^{+0.4}_{-0.4}$	$54.2^{+17.7}_{-11.1}$	0.33/9	peak

from an initial thermal phase to a non-thermal one (GCG03) and a double model fit, i.e. BB+PL, has been used by R04.

We thus systematically analyzed all 15 spectra with both the BB and the PL model (separately and jointly) and report the results in Table 2 and graphically in Fig. 3. The four 'dip' spectra (integrated over 48, 96 and 80 ms for the last two) are best fitted with a PL model without a thermal contribution. The PL photon spectral index is very similar in all four dips, i.e. $\alpha \sim -1.6$. If this corresponds to the photon index α typical of non-thermal spectra found in long, bright GRBs (e.g. Preece et al. 2000), the peak energy should be >1500 keV, i.e. the upper energy limit of the fit window. We note that this spectral slope is consistent with those expected for synchrotron emission from a cooling population of relativistic electrons (such as those accelerated in internal shocks). Interestingly, we also find that the spectrum corresponding to the peak preceding the first dip and between the first and second one is better fitted by a BB+PL model.

In the spectra where both components (BB and PL) contribute to the total photon number, we find that the BB component dominates: it comprises >80 per cent of the total emission during the first peak and >60 per cent during the second one (see Fig. 4).

5 VARIABILITY ESTIMATE

In the previous section it has been shown that the spectral components (thermal and non-thermal) present in GRB 990413 appear to be correlated to the variability of its light curve. In this respect GRB 990413 presents a new, unique phenomenology. The light curves of the other 10 'thermal' bursts are qualitatively smoother than that of GRB 990413, which is instead similar to the majority of GRBs. In this section we quantitatively assess these statements by comparing the variability of GRB 990413 with that of typical non-thermal bursts and with the small sample of the thermal GRBs.

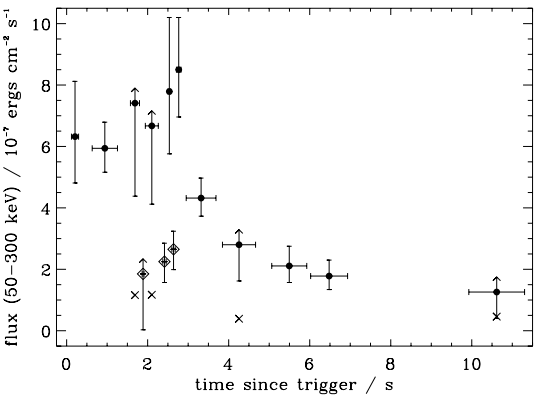

Figure 4. Flux in the 50–300 keV energy band; circles refer to the flux integrated in the time-intervals in which the 'peaks' in the light curve occur and diamonds correspond to flux during 'dips'. The flux in the interval 2.28–2.37 s is not reported because the associated fit normalization is unconstrained. The crosses indicate the contribution of the PL component to the total flux when the best fit comprises a BB superimposed on to a PL component.

In order to evaluate the observed variability we applied the method proposed by Fenimore & Ramirez-Ruiz (2000). We computed the variability as

$$V = \frac{1}{N} \sum_{\rm i} \frac{(c_{\rm i} - \langle c \rangle_w)^2 - (b_{\rm i} + c_{\rm i})}{c_{\rm p}^2}, \quad (1)$$

where $c_{\rm i}$ are the source photon counts (at 64-ms resolution); N is the number of time bins with a signal $> 5\sigma$ above the background; $c_{\rm p}$ is the number of peak counts used for normalization; $\langle c \rangle_w$ are the counts smoothed with the boxcar window of width w. The choice of the time interval for smoothing was determined by the average (observed) thermal phase duration, i.e. w is comparable to or shorter than the time interval in which the thermal spectra were observed (clearly longer time-scales would not reflect the fast fluctuations that we want to sample). We performed several tests and the optimal choice was found to be $w = 3$ s. As the observed time history should be corrected for the cosmological time dilation, we also verified how the result would change if a burst was placed at a typical redshift of $z = 1$: we found – applying the correction as defined in Fenimore & Ramirez-Ruiz (2000) – that the variability changes by less than 10 per cent (the major effect is produced by variations in the smoothing time window).

As the uncertainties on the measured variability V (see Reichart et al. 2001 for the detailed procedure to estimate them) strongly depend on the brightness of the event, for the comparison between GRB 990413 and a larger set of bursts we computed V for a sample of 217 BATSE GRBs of comparable durations ($T_{90} > 10$ s) and peak fluxes (3.7 photons s^{-1} cm^{-2} $< P_{64\,\rm ms} <$ 30.7 photons s^{-1} cm^{-2}). This latter range includes the fluxes measured for GRB 990413 and the bursts analyzed in GCG03. The results are shown in Fig. 5: the variablity of GRB 990413 is clearly similar to the majority of the GRBs in the sample, while it exceeds (by a factor of $\sim$10 in V) the rest of the 'thermal' bursts. We verified that this does not depend on the choice of w, and found that the variability of GRB 990413 increases proportionally to the length of the smoothing time-scale with respect to the other hard-thermal bursts. The five GRBs analyzed by R04 have lower peak fluxes and for the given smoothing time-scale ($w = 3$ s) their variability ranges from $\sim 7 \times 10^{-5}$ to 4×10^{-3} (although with large uncertainties due to the low S/N ratio), i.e. lower than that of GRB 990413.

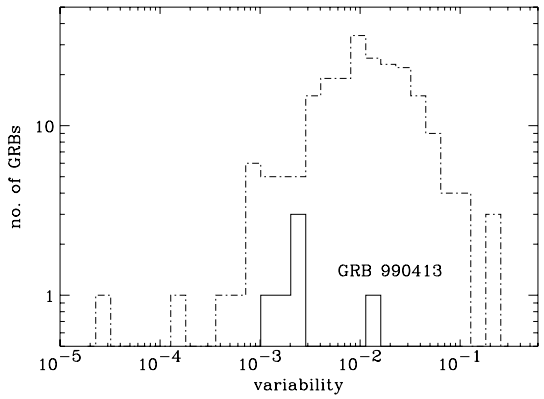

Figure 5. Variability measure for a smoothing time window $w = 3$ s; the dot–dashed histogram represents the sample of 217 GRBs selected within peak flux and duration ranges comprising the values of the bright thermal GRBs (GCG03) and of GRB 990413. GRB 990413 is indicated on the plot.

6 SUMMARY AND DISCUSSION

We presented the time-integrated and the time-resolved spectral analysis of the long duration (14 s) double peaked BATSE burst GRB 990413 that was found to have an extremely hard spectrum. Our analysis indicates that (i) the average spectrum is consistent with thermal emission with typical temperature $kT \sim 70$ keV, comparable to the other 10 'thermal' bursts, and (ii) the spectral evolution of this component is consistent with what found for the thermal GRBs, i.e $kT \propto t^{-1/4}$.

However, we find evidence that a second non-thermal component contributes to the spectrum during the main pulse, in correspondence with the highly variable phase. A combined model (thermal + non-thermal) has been fitted to the time-resolved spectra, showing that: (i) the non-thermal component is present only for about 1 s during the long (14 s) burst, (ii) its slope does not evolve in time and indicates a hard spectrum and (iii) it dominates the flux only during the minima ('dips') of the GRB light curve, while the thermal component dominates for all of the rest of the burst duration.

In the standard GRB fireball model, thermal emission is expected from the expanding fireball when it becomes transparent and typically before the non-thermal particle acceleration in internal shocks occurs. This scenario for the two emission phases can account for an initial thermal spectrum evolving into a non-thermal one, as observed in the 10 GRBs studied by GCG03 and R04. GRB 990413, besides the hard thermal component, revealed a non-thermal contribution still during the (possibly) photospheric phase. Moreover, this component is associated with the rapid temporal variability ($V = 0.016$) that is a result, in the internal shock scenario, of the velocity distribution of the colliding shells within the relativistic outflow. Therefore, any model aimed at accounting for the spectral properties of GRB 990413 needs to allow for the possibility of developing internal shocks (or other forms of dissipation) inside the photosphere (e.g. Daigne & Mochkovitch 2002; Ramirez-Ruiz 2005; Rees & Mészáros 2005; Pe'er, Mészáros & Rees 2006), and has to reproduce consistently the evolution of their relative contributions.

The presence of rapid dips during a thermal-dominated phase is also interesting. Among the possible causes, two appear quite plausible: (i) there might be inhomogeneities in the optical depth of the fireball (at the time of transparency); (ii) the dips directly trace the central engine intermittence in energy injection and launching of the fireball (the duration of the dips still largely exceeds the typical time-scales associated with the fireball formation).

While it is not easy to estimate the percentage of GRBs which may show a detectable thermal component, the fact that GRB 990413 was found independently of its spectral properties may indicate that this phenomenology is more common than known so far. It should be noted that at the brightness level of GRB 990413, the consistency of the spectrum with such a BB-like component is not due to low S/N ratio.

A detailed numerical calculation of the 'transition' to transparency and the formation of internal shocks might clarify the relative roles of the two different radiative regimes and provide information on the physical parameters of the fireball (Lorentz factor distribution of the shells, baryon loading).

ACKNOWLEDGMENTS

It is a pleasure to thank Enrico Ramirez-Ruiz for useful discussions and suggestions. We also thank the referee for constructive comments. This research was supported in part by the National Science Foundation under Grant No. PHY99-07949; the KITP (Santa Barbara) is thanked for kind hospitality (AC). The Italian MIUR and INAF are acknowledged for financial support.

REFERENCES

Band D. L. et al., 1993, ApJ, 413, 281
Crider A., Liang E. P., Smith I. A., 1997, ApJ, 479, L39
Daigne F., Mochkovitch R., 2002, MNRAS, 336, 1271
Fenimore E. E., Ramirez-Ruiz E., 2000, astro-ph/0004176
Ford L. A., 1995, ApJ, 439, 307
Ghirlanda G., Celotti A., Ghisellini G., 2003, A&A, 406, 879
Ghisellini G., Celotti A., 1999, ApJ, 511, L93
Ghisellini G., Celotti A., Lazzati D., 2000, MNRAS, 313, L1
Granot J., Piran T., Sari R., 2000, ApJ, 534, L163
Katz J. I., 1994, ApJ, 432, L107
Lazzati D., Ghisellini G., Celotti A., Rees M. J., 2000, ApJ, 529, L17
Lloyd N. M., Petrosian V., 2002, ApJ, 565, 182
Mészáros P., Rees M. J., 2000, ApJ, 530, 292
Paciesas W. S. et al., 1999, ApJS, 122, 465
Pe'er A., Mészáros P., Rees M. J., 2006, ApJ, 642, 995
Preece R. D., Briggs M. S., Mallozzi R. S., Pendleton G. N., Paciesas W. S., Band D. L., 2000, ApJS, 126, 19
Ramirez-Ruiz E., 2005, MNRAS, 363, L61
Rees M. J., Mészáros P., 1994, ApJ, 430, L93
Rees M. J., Mészáros P., 2005, ApJ, 628, 847
Reichart D. E., Lamb D. Q. Fenimore E. E., Ramirez-Ruiz E., Cline T. L., Hurley K., 2001, ApJ, 552, 57
Ryde F., 2004, ApJ, 614, 827
Tavani M., 1996, ApJ, 466, 768

This paper has been typeset from a TEX/LATEX file prepared by the author.